



Investigation of the sorption characteristics of water lettuce (WL) as a potential low-cost biosorbent for the removal of methyl violet 2B

Linda B.L. Lim^{a,*}, Namal Priyantha^{b,c}, Chin Mei Chan^a, Diyanah Matassan^a,
Hei Ing Chieng^a, Muhammad Raziq Rahimi Kooh^a

^aFaculty of Science, Department of Chemistry, Universiti Brunei Darussalam, Jalan Tungku Link, Gadong, Brunei Darussalam, Tel. +673 8748010; Fax: +673 2461502; email: linda.lim@ubd.edu.bn (L.B.L. Lim), Tel. +673 8665070; email: chinmei.chan@ubd.edu.bn (C.M. Chan), Tel. +673 8853747; email: diyana171@hotmail.com (D. Matassan), Tel. +673 8717770; email: huiing.250@gmail.com (H.I. Chieng), Tel. +673 8658876; email: chernyuan@hotmail.com (M.R.R. Kooh)

^bFaculty of Science, Department of Chemistry, University of Peradeniya, Peradeniya, Sri Lanka, Tel. +94 0718672632; email: namalpriyantha@pdn.ac.lk

^cPostgraduate Institute of Studies, University of Peradeniya, Peradeniya, Sri Lanka

Received 3 July 2014; Accepted 6 February 2015

ABSTRACT

Pistia stratiotes L. (water lettuce or WL) was investigated for its potential as an effective low-cost biosorbent for the removal of methyl violet 2B (MV). Equilibrium isotherm for the adsorption of MV, fitted using six different isotherm models followed by error analyses, indicates that the maximum biosorption capacity (q_{max}) is 0.68 mmol g^{-1} (267.6 mg g^{-1}) and that both the Langmuir and Sips isotherm models lead to good correlation with experimental data. Investigation on effects of pH, ionic strengths, and pre-treatment of the biosorbent on the extent of biosorption indicates the effect of these parameters on MV–biosorbent interaction. Kinetics of the interaction of MV and the biosorbent is fast with more than 50% dye being removed and follows the pseudo-second-order model.

Keywords: *Pistia stratiotes* L.; Water lettuce; Biosorption; Methyl violet 2B; Isotherms; Kinetics

1. Introduction

Dye waste is classified as one of the major pollutants in wastewater, and the industries that utilize chemical dyes frequently are the printing, paper, textile, photography, food, pharmaceutical, and cosmetic industries [1]. These industries may discard their dye wastes into fresh water sources, leading to detrimental effects on the organisms that come into contact with the waste effluents. As such, devising ways of removing dyes from waste discharges and

minimizing the use of synthetic dyes have become increasingly important.

Various wastewater treatment processes, such as coagulation and precipitation, ultrafiltration, ozonation, photocatalytic degradation, electrochemical, and adsorption methods, have been utilized to remove dyes from wastewater [2–4]. Recently, the search for alternative technologies for the removal of environmental pollutants from wastewater has been focused on biosorption which is based on the binding capacities of biosorbents. These biosorbents include fruit waste [5–8], peat [9–13], almond shell [14], pomegranate residual-based activated carbon [15], fungi [16],

*Corresponding author.

black tea leaves [17], and acid-modified wheat bran [18]. The major advantages of biosorption over conventional treatment methods are low cost, high efficiency, minimization of chemical and biological sludge, and regeneration of biosorbent [19].

Aquatic plants are the most popular biosorbents which have been widely used for the removal of pollutants from wastewater [20]. These aquatic biosorbents play a significant role in preserving the purification capability of water and the entire ecosystem. *Pistia stratiotes* L., commonly known as water lettuce (WL), is a free-floating aquatic plant that can be found in shallow waters such as lakes, ponds, and ditches [21]. WL can form dense cover which may cause considerable disruption to the ecosystem [22]. On the other hand, it can compete with algae for nutrients in the water, resulting in decrease in algae growth. The aim of this study is to explore the possibility of utilizing WL for the adsorption of methyl violet dye from industrial discharge. The investigations on parameters such as contact time, dye concentration, kinetics, isotherms, and pH on the adsorption capacity are reported and discussed.

2. Methods

2.1. Chemicals and reagents

A 1,000 mg L⁻¹ stock solution of methyl violet 2B (MV) was prepared by dissolving the dye in distilled water. From this stock solution, a series of dye concentrations ranging from 10 to 1,000 mg L⁻¹ was prepared. MV (C₂₄H₂₈N₃Cl; M_r 393.95 g mol⁻¹) was purchased from Sigma-Aldrich Corporation. Different pH solutions were prepared using NaOH and HNO₃ both of which were purchased from Fluka. All chemicals were used without further purification.

2.2. Materials and sample preparation

The plant samples were collected from a small drain located in Rimba Horticulture Centre in the Brunei-Muara District of Brunei Darussalam. Fresh samples collected were washed several times under running tap water to remove adhering soil and oven dried at 80°C until a constant mass was obtained. The dried sample was then blended and sieved. Particle sizes between 355 and 850 µm were used throughout this study.

2.3. Instrumentation

Shimadzu UV-1601PC UV-vis spectrophotometer was used to measure the absorbance of dye solution

at λ_{\max} of 584.0 nm to determine the concentration of each dye solution, based on a calibration curve, throughout this research, while Shimadzu Model IRPrestige-21FTIR spectrophotometer was used for functional groups determination of adsorbents. Morphological characteristics of the adsorbent surface were investigated using Tescan Vega XMU scanning electron microscope (SEM), and the coating of the adsorbent was done using SPI-MODULETM Sputter Coater. Orbital shaker set at 250 rpm was used in all experiments at room temperature under optimized conditions, unless otherwise stated.

2.4. Determination of the point of zero charge of WL

The initial pH (pH_i) of 50.0 mL of 0.10 M KNO₃ solutions were separately adjusted at pH from 2 to 10 by adding 0.10 M NaOH and 0.10 M HCl. A 0.050 g samples of the biosorbent were separately added to each solution and covered immediately. The suspensions were then shaken at 250 rpm for 24 h. The resulting solution was filtered and the final pH (pH_f) was recorded. The difference between the initial and final pH values ($\Delta\text{pH} = \text{pH}_f - \text{pH}_i$) was plotted against the pH_i. The point of intersection of the resulting curve at which $\Delta\text{pH} = 0$ gave the point of zero charge (pH_{pzc}).

2.5. Optimization of parameters

Biosorption was carried out by shaking 0.050 g of the biosorbent and 50.0 mL of 10 mg L⁻¹ dye solution at 250 rpm. The contact time (shaking and settling) for maximum adsorption was monitored at 30 min interval for 240 min. For the optimum shaking time, each solution was taken out at 30 min interval, filtered, and the remaining dye concentration was determined using Shimadzu UV-vis spectrophotometer. To determine the optimum settling time, the biosorbent was shaken at the optimum shaking time and the contents were allowed to settle. At 30 min interval, each flask was filtered and analyzed as before, and the study was continued up to 240 min. Pre-treatment of the biosorbent by acidification and basification was performed by shaking the biosorbent sample with 1.00 M HNO₃ and 1.00 M NaOH separately for 1 h. The biosorbent was then washed thoroughly with double distilled water and dried in an oven overnight at 80°C. The experiment was then continued by allowing each sample to shake and settle at the optimum shaking and settling times, and then filtered and analyzed as stated earlier. In the study of the effect of medium pH on the adsorption of dye, each biosorbent sample

(0.050 g) was added to 50.0 mL of 10.0 mg L⁻¹ dye solution at different pH values ranging from 2 to 10. The pH was adjusted with 0.10 M NaOH and 0.10 M HCl at room temperature. The flasks were allowed to shake and settle at the pre-determined time periods before it was filtered and analyzed by UV–vis spectrophotometer at λ_{\max} 584.0 nm.

The amount of dye adsorbed per gram of adsorbent at equilibrium, q_e (mmol g⁻¹), was calculated using

$$q_e = \frac{(C_i - C_e) V}{m \times M_r} \quad (1)$$

where C_i is the initial dye concentration (mg L⁻¹), C_e is the equilibrium dye concentration (mg L⁻¹), V is the volume of the dye solution (L), m is the mass of WL (g), and M_r is the molecular weight of MV.

The percentage removal of the dye is represented by:

$$\text{Removal (\%)} = \frac{(C_i - C_e) \times 100\%}{C_i} \quad (2)$$

2.6. Effect of ionic strength

Effect of ionic strength was determined by monitoring the extent of dye removal when 0.050 g of WL was separately mixed with 25.0 mL of 100 mg L⁻¹ dye solution that had been prepared in KNO₃ medium of different concentrations ranging from 0.001 to 0.80 M. These experiments were carried out by shaking the above mixtures for the optimum shaking and settling times at room temperature on an orbital shaker at 250 rpm.

2.7. Isotherm analysis

Samples of 0.100 g biosorbent were separately mixed with 50.0 mL dye solution of various concentrations ranging from 0 to 1,000 mg L⁻¹. Each mixture was shaken at 250 rpm and allowed to settle for a pre-determined time period. The mixture was filtered and the concentration of the dye in the filtrate was determined using UV–vis spectral measurements.

2.8. Kinetics studies of biosorption

Samples of 0.040 g biosorbent were individually placed in separate flasks and 20.0 mL of dye solution with initial dye concentrations (C_i) of 100 mg L⁻¹ was introduced to each flask. The mixture was shaken at 250 rpm at room temperature for different reaction

times, and the residual dye concentration in the filtrate was determined using UV–vis spectral measurements. The same procedure was repeated for dye concentrations of 200, 300, and 400 mg L⁻¹.

2.9. Theoretical aspects of isotherm and kinetics studies

Six different isotherm models, namely the Langmuir [23], Freundlich [24], Temkin [25], Dubinin–Radushkevich (D–R) [26], Redlich–Peterson (R–P) [27], and Sips [28], were used to determine the biosorption characteristics (Table 1). Various error analyses [29–31] were also performed on these isotherm models (Table 2).

The kinetics models, such as the pseudo-first-order, pseudo-second-order and intraparticle diffusion, were used to investigate the adsorption kinetics and the rate-limiting step for the adsorption of WL on MV.

The pseudo-first-order is commonly expressed as:

$$\log(q_e - q_t) = \log(q_e) - \frac{k_1}{2.303} t \quad (3)$$

where q_t is the amount of adsorbate adsorbed per gram of adsorbent (mmol g⁻¹) at time t , k_1 is the pseudo-first-order rate constant (min⁻¹), and t is the time shaken (min). Parameter k_1 is calculated from the linear plot of $\log(q_e - q_t)$ vs. t .

The pseudo-second-order is expressed as:

$$\frac{t}{q_t} = \frac{1}{q_e^2 k_2} + \frac{t}{q_e} \quad (4)$$

where k_2 is pseudo-second-order rate constant (g mmol⁻¹ min⁻¹). Parameter k_2 can be obtained from the linear plot of $\frac{t}{q_t}$ vs. t .

The Weber Morris intraparticle diffusion model was applied to understand the adsorption of MV from the exterior surface to the pores of WL. The Weber Morris intraparticle diffusion equation is expressed as:

$$q_t = k_{id} t^{1/2} + C \quad (5)$$

where k_{id} is the intraparticle diffusion rate constant (mmol g⁻¹ min^{-1/2}) and C is the intercept that is associated with the thickness of the boundary layer. k_{id} and C can be calculated from the linear plot of q_t vs. $t^{1/2}$.

3. Results and discussion

3.1. SEM characterization of WL

The surface morphology of WL investigated through SEM images reveals that the WL surface

Table 1
Different isotherm models

Isotherm model	Non-linear	Linear	Plot
Langmuir	$q_e = \frac{K_L C_e q_{\max}}{1 + K_L C_e}$	$\frac{C_e}{q_e} = \frac{1}{K_L q_{\max}} + \frac{C_e}{q_{\max}}$	C_e/q_e vs. C_e
Freundlich	$q_e = K_F C_e^{\frac{1}{n}}$	$\ln q_e = \frac{1}{n} \ln C_e + \ln K_F$	$\ln q_e$ vs. $\ln C_e$
Temkin	$q_e = \frac{RT}{b} \ln K_T C_e$ where $B = \frac{RT}{b}$	$q_e = B \ln K_T + B \ln C_e$	q_e vs. $\ln C_e$
D-R	$q_e = q_{\max} \exp(-\beta \varepsilon^2)$; $\varepsilon = RT \ln \left[1 + \frac{1}{C_e} \right]$; $E = \frac{1}{\sqrt{2\beta}}$	$\ln q_e = \ln q_{\max} - \beta \varepsilon^2$	$\ln q_e$ vs. ε^2
R-P	$q_e = \frac{K_R C_e}{1 + a_R C_e}$	$\ln \left(K_R \frac{C_e}{q_e} - 1 \right) = \alpha \ln C_e + \ln a_R$ where $0 \leq \alpha \leq 1$	$\ln \left(K_R \frac{C_e}{q_e} - 1 \right)$ vs. $\ln C_e$
Sips	$q_e = \frac{q_{\max} K_s C_e^{\frac{1}{n}}}{1 + K_s C_e^{\frac{1}{n}}}$	$\ln \left(\frac{q_e}{q_{\max} - q_e} \right) = \frac{1}{n} \ln C_e + \ln K_s$	$\ln \left(\frac{q_e}{q_{\max} - q_e} \right)$ vs. $\ln C_e$

Table 2
List of error functions

Type of errors	Equations
Average relative error (ARE)	$\frac{100}{n} \sum_{i=1}^n \left \frac{q_{e,\text{meas}} - q_{e,\text{calc}}}{q_{e,\text{meas}}} \right _i$
Sum square error (ERRSQ/SSE)	$\sum_{i=1}^n (q_{e,\text{calc}} - q_{e,\text{meas}})_i^2$
Hybrid fractional error function (HYBRID)	$\frac{100}{n-p} \sum_{i=1}^n \left[\frac{(q_{e,\text{meas}} - q_{e,\text{calc}})^2}{q_{e,\text{meas}}} \right]_i$
Sum of absolute error (EABS)	$\sum_{i=1}^n q_{e,\text{meas}} - q_{e,\text{calc}} $
Marquardt's percent standard deviation (MPSD)	$100 \sqrt{\frac{1}{n-p} \sum_{i=1}^n \left(\frac{q_{e,\text{meas}} - q_{e,\text{calc}}}{q_{e,\text{meas}}} \right)^2}$
Non-linear chi-square test (χ^2)	$\sum_{i=1}^n \frac{(q_{e,\text{calc}} - q_{e,\text{meas}})^2}{q_{e,\text{meas}}}$

Note: $q_{e,\text{calc}}$ and $q_{e,\text{meas}}$ are the calculated and measured adsorption capacity, respectively; n is the number of data points; p is the number of parameters.

consists of pores and cavities of various sizes which are able to provide large surface area for adsorption of dyes (Fig. 1(A)). Fig. 1(B) shows a significant change in the structure of the WL surface as a result of dye adsorption, whereby the surface becomes less rough with the pores and cavities being covered with the dye.

3.2. Effect of contact time

Contact time, i.e. shaking and settling times, plays a significant role in wastewater treatment by adsorption as the efficiency depends on rapid uptake of biosorbent and establishment of equilibrium in short period of time. The adsorption of MV dye on WL was investigated as a function of contact time. Fig. 2 shows rapid removal of MV within the first 30 min with approximately 69, 63, 48, and 50% of MV being adsorbed at initial concentrations of 100, 200, 300, and 400 mg L⁻¹, respectively. The high initial rate of dye

removal is due to the abundant availability of adsorption sites on the biosorbent surface. As more dyes are adsorbed overtime, the adsorption becomes less efficient as the number of available sites on WL decreases until finally an equilibrium is reached.

Although the time taken to reach equilibrium depends on the concentration of the dye as observed in Fig. 2, it is reasonable to assume that a time common shaking period of 180 min can be taken as the optimum time to reach equilibrium for all concentrations attempted. This is comparable with other low-cost biosorbents reported as shown in Table 3.

With known optimized shaking time, the adsorbent with dye solution was allowed to settle for a period of time to ensure full equilibrium is reached. During settling (resting), the adsorption system would undergo various diffusion or mass transfers steps, which are relatively slow processes [11,35]. The settling time required for WL to attain equilibrium was determined to be 90 min. Hence, the shaking time was

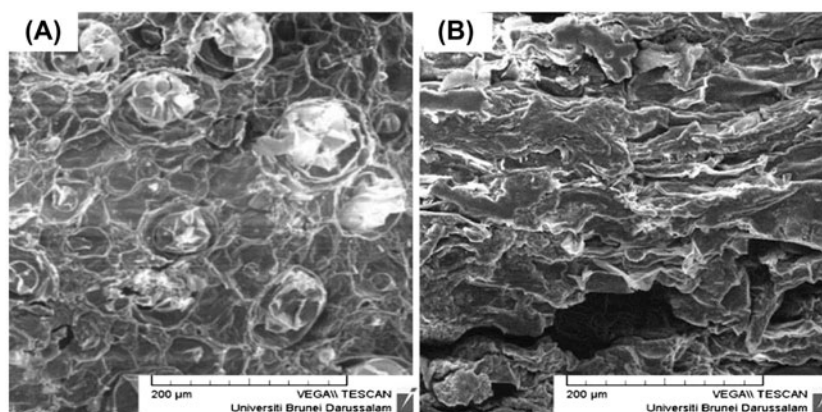


Fig. 1. SEM images of WL: (A) before adsorption and (B) after adsorption with MV dye.

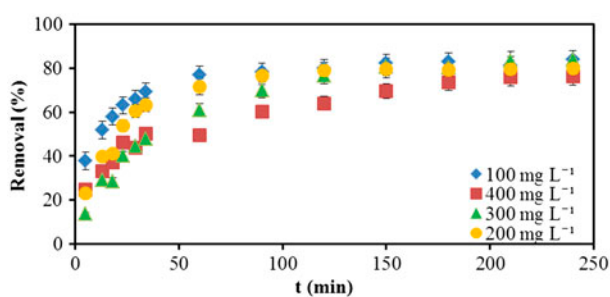


Fig. 2. Effect of shaking time of WL with MV (initial dye concentration: 100, 200, 300, and 400 mg L⁻¹; temperature: 298 K; pH: 6.0).

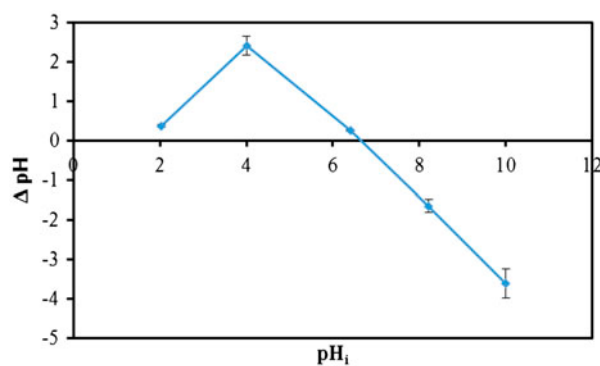


Fig. 3. Point of zero charge of WL.

Table 3

Comparison of shaking time for various low-cost biosorbents

Adsorbent	Shaking time (min)	References
Water lettuce	180	This work
Palm kernel fiber	140	[32]
Sunflower seed hull	135	[33]
<i>Phragmites australis</i>	150–240	[34]

chosen as 180 min followed by 90 min settling time for all the subsequent studies.

3.3. Point of zero charge

The point of zero charge (pH_{pzc}) of WL was found to be at approximately pH 6.5 (Fig. 3), indicating that the surface charge would be zero at this pH. Hence, the surface of adsorbent would be predominantly positively charged at pH lower than pH_{pzc} , and the

surface would be predominantly negatively charged if the pH was made greater than the pH_{pzc} .

3.4. Effect of medium pH

The influence of pH on the removal of dye was studied to gain further insight into the adsorption process while concentration of dye, amount of biosorbent, and temperature were fixed at 10 mg L⁻¹ (0.050 g WL, 50.0 mL MV) and 298 K, respectively, at the pre-determined shaking and settling times of the biosorbent. At normal pH of 6.0, the amount of MV being removed was 85%. When the pH was adjusted to strongly acidic conditions, the adsorption capacity of WL was significantly decreased (Fig. 4). This is probably due to the positive charge of the surface of WL at pH below the pH_{pzc} of 6.5, at which cationic dye molecules would not be attracted to the adsorbent surface. The decrease in adsorption of MV could also be attributed to the presence of a large concentration of hydrogen ions in strongly acidic medium which may compete with the

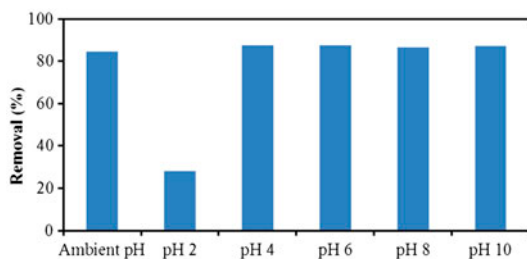


Fig. 4. Effect of medium pH on biosorption of MV on WL (initial dye concentration: 10 mg L^{-1} ; temperature: 298 K).

cationic MV dye molecules for the adsorption sites of the biosorbent [36]. At increasing pH (pH 4–10), the biosorbent would become more negatively charged enhancing the positively charged MV ions through electrostatic forces of attraction, thus causing the adsorption capacity to increase [2]. Under experimental condition employed, no significant increase was observed at pH 4–10, similar to the adsorption of MV using duckweed [37] and tarap peel [6]. As the results reported show that the normal pH gave reasonably high adsorption of MV dye, no pH adjustment was required for effective removal of MV.

3.5. Effect of pre-treatment of biosorbent

The effectiveness of the biosorbent toward the attraction of MV is decreased by about 9% upon the treatment with 1.00 M nitric acid (Fig. 5). This could be due to the protonation of surface resulting in repulsion between the positively charged surface of WL with cationic MV dye. On the other hand, treatment with 1.00 M NaOH increased the dye removal ability of MV by 8%. Deprotonation with NaOH would cause the surface to be more negatively charged thereby favoring adsorption of the cationic MV dye. It can thus be stated that the usage of higher pH could provide a means of improving the adsorption

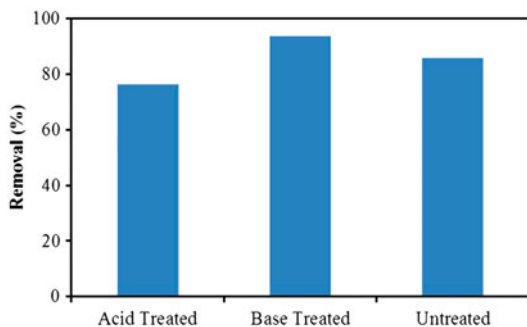


Fig. 5. Effect of pre-treatment of WL on biosorption of MV.

efficiency of MV dye on WL. However, complex pre-treatment procedures of WL were not attempted as the untreated WL was able to efficiently remove MV with approximately 85% removal.

3.6. Effect of ionic strength

Introduction of an ionic atmosphere with KNO_3 reduced the extent of removal of MV by 24% at 0.001 M KNO_3 concentration (Fig. 6). When the concentration was changed from 0.001 to 0.80 M KNO_3 solution, the effect of ionic strength did not significantly influence the removal of MV. A decrease in the adsorption suggests that there is electrostatic force of attraction between WL and MV. This could be due to the interaction between MV dye and K^+ ions for the sites available for adsorption [2,38]. However, the ionic strength did not seem to have an overly strong influence on the adsorption of MV on WL as shown by the slight changes at other concentrations.

3.7. Adsorption isotherms

In order to understand the biosorption system of MV on WL, equilibrium isotherm was carried out with initial dye concentrations ranging from 0 to $1,000 \text{ mg L}^{-1}$ at normal temperature. Fig. 7 shows the equilibrium isotherm of q_e vs. the dye concentration at equilibrium (C_e). Six different isotherm models listed in Table 1 were used to understand the adsorption characteristics between the WL and MV at equilibrium. Various error analyses (Table 2) were also performed to obtain the most suitable adsorption isotherm model to describe the whole adsorption process.

The Langmuir isotherm assumes that when adsorption takes place onto the surface at the active site of the adsorbent, no further adsorption will occur

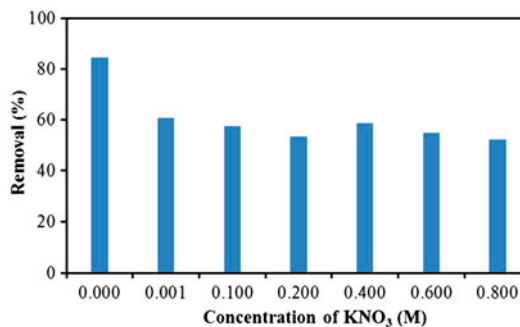


Fig. 6. Effect of ionic strength of WL on biosorption of MV (initial dye concentration: 100 mg L^{-1} , temperature: 298 K).

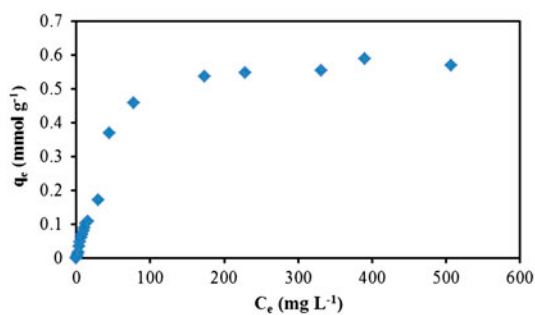


Fig. 7. Adsorption isotherm of MV onto WL.

at that site [23]. The energies of adsorption on the surface are uniform and adsorbate does not transigrate in the plane of the surface of adsorbent. Temkin isotherm assumes the heat of adsorption decreases linearly with the surface coverage due to the uniform distribution of the binding energies [25]. The D–R isotherm assumes no homogenous surface of the adsorbent [26]. The mean energy (E) of the sorption per molecule of sorbate can be calculated from the constant (β). The R–P [27] and Sips [28] isotherms are three-parameter isotherm models which incorporate both the Langmuir and Freundlich isotherms into a single equation. Both R–P and Sips isotherms can be calculated using a minimization procedure through maximizing the R^2 of the linear plot. The R–P isotherm reduces to the Freundlich isotherm when $\alpha=1$ and to Henry's equation when $\alpha=0$. The Sips isotherm model is used for heterogeneous adsorption systems which reduces to the Langmuir isotherm at high concentration, and to the Freundlich model at low concentration.

The Langmuir isotherm can be defined as a dimensionless constant separation factor or equilibrium parameter [39], (R_L), which was used to describe the nature of adsorption; $R_L > 1$ being unfavorable, $0 < R_L < 1$ is favorable, while $R_L = 0$ being irreversible.

$$R_L = \frac{1}{1 + K_L C_0} \quad (6)$$

The R_L value for initial concentration of MV at $1,000 \text{ mg L}^{-1}$ was 0.08 indicating that the adsorption of MV onto WL was favorable.

The D–R isotherm was used to calculate the adsorption free energy (E). The degree of the adsorption could be characterized as chemical if the value E lies between 8 and 16 kJ mol^{-1} or physical if E is less than 8 kJ mol^{-1} . The E for WL was 0.88 kJ mol^{-1} ($881.46 \text{ J mol}^{-1}$), suggesting that the adsorption of MV on WL is a physisorption process.

Based on the results obtained for coefficient of correlation (R^2) (Table 4), the six error analyses (Table 5) together with simulated isotherms (figure not shown), the Freundlich, D–R, and R–P models were found to give a poor fit when compared to the experimental data. This was reflected in their large errors especially for D–R (Table 5). Even though the Temkin isotherm showed good simulated isotherm with $R^2 = 0.9299$, its errors were large especially for ARE and MPSD, indicating the unsuitability of the Temkin model.

Of the six isotherm models used, both the Langmuir and Sips isotherms gave the best fit for adsorption of MV on WL with $R^2 = 0.9863$ and 0.9857 , respectively. Both isotherm models gave compatible results with the Sips isotherm having smaller overall errors despite it having a lower R^2 than the Langmuir. The q_{\max} obtained from the Langmuir isotherm was found to be 0.68 mmol g^{-1} (267.6 mg g^{-1}) for MV, while the Sips isotherm gave a q_{\max} of 0.62 mmol g^{-1} (244.2 mg g^{-1}), a difference of less than 40 mg g^{-1} .

Table 4
Parameters for various isotherm models

Model	Water lettuce (WL)
<i>Langmuir</i>	
q_{\max} (mmol g ⁻¹)	0.68
K_L (L mmol ⁻¹)	0.01
R^2	0.9863
R_L	0.08
<i>Freundlich</i>	
K_F (mmol g ⁻¹)	0.01
n	1.39
R^2	0.9139
<i>Temkin</i>	
K_T (L mmol ⁻¹)	0.34
b (J mol ⁻¹)	21,376
R^2	0.9299
<i>Dubinin–Radushkevich</i>	
q_{\max} (mmol g ⁻¹)	0.32
B (J mol ⁻¹)	6.44×10^{-7}
E (J mol ⁻¹)	881.46
R^2	0.8641
<i>Redlich–Peterson</i>	
K_R	0.02
α	0.43
a_R	0.65
R^2	0.7661
<i>Sips</i>	
q_{\max} (mmol g ⁻¹)	0.62
K_S (L mmol ⁻¹)	0.01
$1/n$	1.20
n	0.83
R^2	0.9857

Table 5
Parameters for isotherm models and error analyses

Model	R^2	ARE	ERRSQ/SSE	HYBRID	EABS	MPSD	χ^2
Langmuir	0.9863	10.91	0.03	0.44	0.41	17.11	0.07
Freundlich	0.9139	29.61	0.48	5.46	1.68	38.45	0.93
Temkin	0.9299	78.19	0.06	5.84	0.87	189.66	0.99
D–R	0.8641	273.86	0.78	58.94	3.62	443.91	10.02
R–P	0.7661	23.48	0.33	3.90	1.36	34.34	0.62
Sips	0.9857	9.04	0.01	0.32	0.32	13.87	0.05

It can be seen in Table 6 that WL, with its high q_{\max} , has the potential to act as a low-cost biosorbent for the removal of MV when compared to most other reported biosorbents. When compared to banana peel and orange peel, its q_{\max} is almost 30 times higher. WL is almost 2–3 times more effective than adsorbents, such as halloysite nanotubes and nanocellulose hydrogel. The WL used in this study, apart from oven drying, was not chemically treated. As shown in the pre-treatment study, its adsorption capacity could be further enhanced through chemical modification, such as basification.

3.8. Kinetics of biosorption

The kinetics of biosorption of MV on WL was analyzed using the pseudo-first-order [45], pseudo-second-order [46], and the Weber Morris intraparticle diffusion [47] models. The coefficient of determination, R^2 , obtained for pseudo-second-order for all four initial concentrations of 100, 200, 300, and 400 mg L⁻¹

were 0.9998, 0.9985, 0.9980, and 0.9910, respectively (Table 7, Fig. 8(A)), while the majority of data for pseudo-first-order did not fall into straight lines (figure not shown) and yield R^2 of 0.8906, 0.8293, 0.9882, and 0.9022. Moreover, the $q_{e,calc}$ values obtained from pseudo-second-order were much closer to the $q_{e,exp}$ than values obtained from pseudo-first-order (Table 7). Hence, when the R^2 and the values of $q_{e,calc}$ were taken into consideration, it can be concluded that the pseudo-second-order best described the kinetic data, indicating that the adsorption may be governed by a chemical process.

The Weber Morris intraparticle diffusion model, which explains the diffusion behavior of adsorption, usually shows three phases: the fast external diffusion, followed by gradual surface adsorption owing to the intraparticle diffusion, and lastly, the slow equilibrium phase [48,49]. The multi-linearity observed in the linear plot of Weber Morris model shown in Fig. 8(B) indicates that the fast external surface adsorption is quick and completed within 25 min. Özacar and

Table 6
Comparison of maximum adsorption capacities of various biosorbents

Adsorbent	q_{\max} (mg g ⁻¹)	References
<i>Pistia stratiotes</i> L.	267.6	This work
Orange peel	11.5	[29]
Banana peel	12.2	[29]
Palm kernel fiber	140	[32]
Sunflower seed hull	92.6	[33]
Halloysite nanotubes	113.6	[30]
Fe ₃ O ₄ magnetite nanoparticles	416.7	[31]
Fruit waste residue	27.8	[40]
Pu-erh Tea powder	277.8	[41]
<i>Posidonia oceanica</i> (L.) leaf	119.1	[42]
Almond shell	76.3	[43]
<i>Casuarina equisetifolia</i> needle	165.0	[44]
Tarap (<i>Artocarpus odoratissimus</i>) peel	137.3	[6]
Duckweed	332.5	[37]

Table 7
Parameters for various kinetic models

Model	Parameters	Concentration (mg L ⁻¹)			
		100	200	300	400
Pseudo-first-order	$q_{e,exp}$ (mmol g ⁻¹)	0.11	0.21	0.33	0.42
	k_1 (min ⁻¹)	0.02	0.02	0.02	0.02
	$q_{e,calc}$ (mmol g ⁻¹)	0.04	0.10	0.27	0.35
	R^2	0.8906	0.8293	0.9882	0.9022
Pseudo-second-order	k_2 (g mmol ⁻¹ min ⁻¹)	1.39	0.33	0.09	0.09
	$q_{e,calc}$ (mmol g ⁻¹)	0.11	0.23	0.37	0.45
	R^2	0.9998	0.9985	0.9980	0.9910
Intraparticle diffusion	Region A				
	k_{id} (mmol g ⁻¹ min ^{-1/2})	0.096	0.024	0.033	0.027
	C	0.031	0.017	0.002	0.088
	R^2	0.9101	0.9182	0.9689	0.8421
	Region B				
	k_{id} (mmol g ⁻¹ min ^{-1/2})	0.001	0.003	0.011	0.019
	C	0.100	0.173	0.176	0.140
	R^2	0.7983	0.6678	0.8715	0.9561

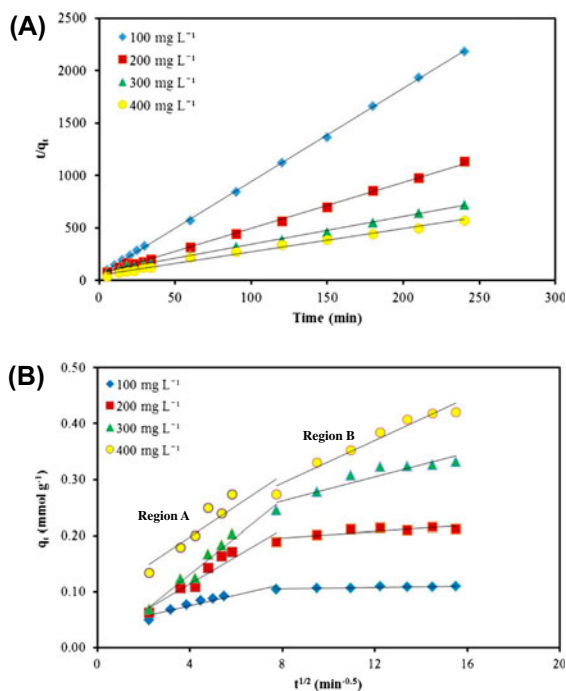


Fig. 8. (A) The pseudo-second-order kinetics, and (B) Weber Morris intraparticle diffusion model plot for 100, 200, 300, and 400 mg L⁻¹ MV into WL. (Region A represented the gradual surface adsorption owing to intraparticle diffusion, while region B represented the slow equilibrium phase.)

Şengil observed a similar trend in the adsorption of disperse dye into alunite [49]. None of the linear sections passed through the origin, indicating that

although the intraparticle phase is present, it is not the rate-limiting step, suggesting the involvement of other mechanisms [34].

3.9. FTIR spectral studies of WL

Functional group characterization of WL using FTIR showed the presence of hydroxyl and amino groups in the wavelength at 3,342 cm⁻¹ for both untreated and treated WL (Fig. 9). The peaks at 2,918 and 2,850 cm⁻¹ are the asymmetric stretches of -CH group. The presence of the peak at wavelength 1,640 cm⁻¹ indicates the presence of C=O. Upon

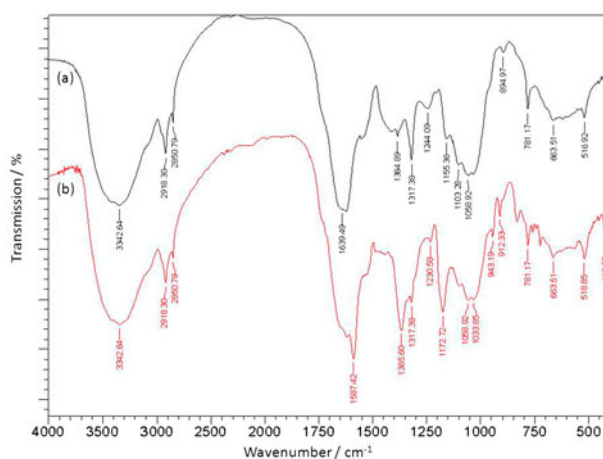


Fig. 9. FTIR of WL (a) untreated and (b) after adsorption with MV.

treatment with MV, the peak at $1,384\text{ cm}^{-1}$ shifted to $1,366\text{ cm}^{-1}$ and become sharper. This peak could be attributed to the -COO- symmetric stretching [50]. The new band formed at $1,172\text{ cm}^{-1}$ is indicative of the presence C–N stretching in MV. These changes suggested strong interaction between MV and functional groups of phenolic -OH and -COO- present on WL. Hence, the carboxylic acid group, the main functional group in WL involved in the binding, plays a significant role in the adsorption of MV on WL. The band at $1,033\text{ cm}^{-1}$ represents the bending vibration of -OH group and stretching vibration of C–O–C in the lignin structure of WL. This observation is similar to the observation reported in the adsorption of MV by biochar derived from crop residues [51].

4. Conclusion

In this study, WL was successfully utilized as a low-cost biosorbent for the removal of cationic dye, MV. The adsorption isotherm for MV was found to fit both the Langmuir and Sips isotherm models. The maximum adsorption capacity (q_{max}) for MV was 267.6 mg g^{-1} according to the Langmuir isotherm model, which is either comparable or better than some reported biosorbents, demonstrating that WL has the potential to be used as a low-cost biosorbent for the removal of MV dye. Investigation of kinetics shows the validity of the pseudo-second-order model with an apparent rate constant of $1.39\text{ g mmol}^{-1}\text{ min}^{-1}$ for 100 mg L^{-1} initial dye concentration.

Acknowledgments

The authors would like to thank the Government of Brunei Darussalam and the Universiti Brunei Darussalam for their financial support. The authors are also grateful to the CAMES and the Department of Biology at UBD for the use of SEM.

References

- [1] G. Crini, Non-conventional low-cost adsorbents for dye removal: A review, *Bioresour. Technol.* 97 (2006) 1061–1085.
- [2] N. Gupta, A.K. Kushwaha, M.C. Chattopadhyaya, Application of potato (*Solanum tuberosum*) plant wastes for the removal of methylene blue and malachite green dye from aqueous solution, *Arab. J. Chem.* (2011), doi: [10.1016/j.arabjc.2011.07.021](https://doi.org/10.1016/j.arabjc.2011.07.021).
- [3] S.I. Abou-Elela, M.A. El-Khateeb, Treatment of ink wastewater via heterogeneous photocatalytic oxidation, *Desalin. Water Treat.* 7 (2009) 1–5.
- [4] R. Singh, Production of high-purity water by membrane processes, *Desalin. Water. Treat.* 3 (2009) 99–110.
- [5] N. Priyantha, L.B.L. Lim, D.T.B. Tennakoon, N.H.M. Mansor, M.K. Dahri, H.I. Chieng, Breadfruit (*Artocarpus altilis*) waste for bioremediation of Cu(II) and Cd (II) Ions from aqueous medium, *Ceylon J. Sci.* 17 (2013) 19–29.
- [6] L.B.L. Lim, N. Priyantha, H.I. Chieng, M.K. Dahri, D.T.B. Tennakoon, T. Zehra, M. Suklueng, *Artocarpus odoratissimus* skin as a potential low-cost biosorbent for the removal of methylene blue and methyl violet 2B, *Desalin. Water Treat.* 53 (2015) 964–975, doi: [10.1080/19443994.2013.852136](https://doi.org/10.1080/19443994.2013.852136).
- [7] L.B.L. Lim, N. Priyantha, D.T.B. Tennakoon, H.I. Chieng, M.K. Dahri, M. Suklueng, Breadnut peel as a highly effective low-cost biosorbent for methylene blue: Equilibrium, thermodynamic and kinetic studies, *Arab. J. Chem.* (2014), doi: [10.1016/j.arabjc.2013.12.018](https://doi.org/10.1016/j.arabjc.2013.12.018).
- [8] L.B.L. Lim, N. Priyantha, D.T.B. Tennakoon, M.K. Dahri, Biosorption of cadmium(II) and copper(II) ions from aqueous solution by core of *Artocarpus odoratissimus*, *Environ. Sci. Pollut. Res.* 19 (2012) 3250–3256.
- [9] L.B.L. Lim, N. Priyantha, D.T.B. Tennakoon, H.I. Chieng, C. Bandara, Sorption characteristics of peat of Brunei Darussalam I: Characterization of peat and adsorption equilibrium studies on methylene blue—Peat interactions, *Ceylon J. Sci.* 17 (2013) 41–51.
- [10] L.B.L. Lim, N. Priyantha, D.T.B. Tennakoon, T. Zehra, Sorption characteristics of peat of Brunei Darussalam. II: Interaction of aqueous copper(II) species with raw and processed peat, *J. Ecotechn. Res.* 17 (2013) 45–49.
- [11] H.I. Chieng, L.B.L. Lim, N. Priyantha, Sorption characteristics of peat from Brunei Darussalam for the removal of rhodamine B dye from aqueous solution: Adsorption isotherms, thermodynamics, kinetics and regeneration studies, *Desalin. Water Treat.* (2014), doi: [10.1080/19443994.2014.919609](https://doi.org/10.1080/19443994.2014.919609).
- [12] H.I. Chieng, T. Zehra, L.B.L. Lim, N. Priyantha, D.T.B. Tennakoon, Sorption characteristics of peat of Brunei Darussalam IV: Equilibrium, thermodynamics and kinetics of adsorption of methylene blue and malachite green dyes from aqueous solution, *Environ. Earth Sci.* 72 (2014) 2263–2277.
- [13] H.I. Chieng, L.B.L. Lim, N. Priyantha, Enhancing adsorption capacity of toxic malachite green dye through chemically modified breadnut peel: Equilibrium, thermodynamics, kinetics and regeneration studies, *Environ. Technol.* 36 (2014) 86–97.
- [14] M. Fat'hi, A. Asfaram, A. Hadipour, M. Roosta, Kinetics and thermodynamic studies for removal of acid blue 129 from aqueous solution by almond shell, *J. Environ. Health Sci. Eng.* 12 (2014) 62–68.
- [15] E. Radaei, M. Alavi Moghaddam, M. Arami, Removal of reactive blue 19 from aqueous solution by pomegranate residual-based activated carbon: Optimization by response surface methodology, *J. Environ. Health Sci. Eng.* 12 (2014) 65–72.
- [16] H. Akdogan, M. Topuz, A. Urhan, Studies on decolorization of reactive blue 19 textile dye by *Coprinus plicatilis*, *J. Environ. Health Sci. Eng.* 12 (2014) 49–55.
- [17] M. Hossain, M. Alam, Adsorption kinetics of Rhodamine-B on used black tea leaves, *Iran. J. Environ. Health Sci. Eng.* 9 (2012) 2–8.
- [18] S. Yao, H. Lai, Z. Shi, Biosorption of methyl blue onto tartaric acid modified wheat bran from aqueous solution, *Iran. J. Environ. Health Sci. Eng.* 9 (2012) 16–21.

- [19] U. Farooq, J.A. Kozinski, M.A. Khan, M. Athar, Biosorption of heavy metal ions using wheat based biosorbents—A review of the recent literature, *Bioresour. Technol.* 101 (2010) 5043–5053.
- [20] Y. Zimmels, F. Kirzhner, A. Malkovskaja, Application of *Eichhornia crassipes* and *Pistia stratiotes* for treatment of urban sewage in Israel, *J. Environ. Manage.* 81 (2006) 420–428.
- [21] N.M. Tarlyn, T.A. Kostman, P.A. Nakata, S.E. Keates, V.R. Franceschi, Axenic culture of *Pistia stratiotes* for use in plant biochemical studies, *Aquat. Bot.* 60 (1998) 161–168.
- [22] Y. Zimmels, F. Kirzhner, A. Malkovskaja, Application and features of cascade aquatic plants system for sewage treatment, *Ecol. Eng.* 34 (2008) 147–161.
- [23] I. Langmuir, The constitution and fundamental properties of solids and liquids. II. Liquids. 1, *J. Am. Chem. Soc.* 39 (1917) 1848–1906.
- [24] H. Freundlich, Over the adsorption in the solution, *J. Phys. Chem.* 57 (1906) 385–470.
- [25] M.J. Temkin, V. Pyzhev, Kinetics of ammonia synthesis on promoted iron catalysts, *J. Phys. Chem.* 57 (1906) 327–356.
- [26] M.M. Dubinin, L.V. Radushkevich, Equation of the characteristic curve of activated charcoal, *Proc. Acad. Sci.* 55 (1947) 331–337.
- [27] O. Redlich, D.L. Peterson, A useful adsorption isotherm, *J. Phys. Chem.* 63 (1959) 1024–1029.
- [28] R. Sips, On the structure of a catalyst surface, *J. Chem. Phys.* 16 (1948) 490–495.
- [29] G. Annadurai, R. Juang, D. Lee, Use of cellulose-based wastes for adsorption of dyes from aqueous solutions, *J. Hazard. Mater.* 92 (2002) 263–274.
- [30] R. Liu, B. Zhang, D. Mei, H. Zhang, J. Liu, Adsorption of methyl violet from aqueous solution by halloysite nanotubes, *Desalination* 268 (2011) 111–116.
- [31] F. Keyhanian, S. Shariati, M. Faraji, M. Hesabi, Magnetite nanoparticles with surface modification for removal of methyl violet from aqueous solutions, *Arab. J. Chem.* (2011), doi: [10.1016/j.arabjc.2011.04.012](https://doi.org/10.1016/j.arabjc.2011.04.012).
- [32] A.E. Ofomaja, E.E. Ukpabor, S.A. Uzoekwe, Biosorption of methyl violet onto palm kernel fiber: Diffusion studies and multistage process design to minimize biosorbent mass and contact time, *Biomass Bioenergy* 35 (2011) 4112–4123.
- [33] B.H. Hameed, Equilibrium and kinetic studies of methyl violet sorption by agricultural waste, *J. Hazard. Mater.* 154 (2008) 204–212.
- [34] S. Chen, J. Zhang, C. Zhang, Q. Yue, Y. Li, C. Li, Equilibrium and kinetic studies of methyl orange and methyl violet adsorption on activated carbon derived from *Phragmites australis*, *Desalination* 252 (2010) 149–156.
- [35] L.B.L. Lim, N. Priyantha, U.K. Ramli, H.I. Chieng, Adsorption of Cd(II) ions using Lamiding, a wild vegetable from Brunei Darussalam, *J. Appl. Phytotechnol. Environ. Sanit.* 3 (2014) 65–74.
- [36] W. Hassan, U. Farooq, A. Muhammad, A. Makshoof, A.K. Misbahul, Potential biosorbent, *Haloxylon recurvum* plant stems, for the removal of methylene blue dye, *Arab. J. Chem.* (2013), doi: [10.1016/j.arabjc.2013.05.002](https://doi.org/10.1016/j.arabjc.2013.05.002).
- [37] L.B.L. Lim, N. Priyantha, C. Chan, D. Matassan, H. Chieng, M.R.R. Kooch, Adsorption behavior of methyl violet 2B using Duckweed: Equilibrium and kinetics studies, *Arab. J. Sci. Eng.* 39 (2014) 6757–6765.
- [38] O. Hamdaoui, F. Saoudi, M. Chiha, E. Naffrechoux, Sorption of malachite green by a novel sorbent, dead leaves of plane tree: Equilibrium and kinetic modeling, *Chem. Eng. J.* 143 (2008) 73–84.
- [39] T.W. Weber, R.K. Chakravorti, Pore and solid diffusion models for fixed-bed adsorbers, *J. Am. Inst. Chem. Eng.* 20 (1974) 228–238.
- [40] P. Parimaladevi, V. Venkateswaran, Kinetics, thermodynamics and isotherm modelling of adsorption of triphenylmethane dyes (methyl violet, malachite green and magenta II) on to fruit waste, *J. Appl. Sci. Tech. Environ. Sanit.* 1 (2011) 273–283.
- [41] P. Li, Y. Su, Y. Wang, B. Liu, L. Sun, Bioadsorption of methyl violet from aqueous solution onto Pu-erh tea powder, *J. Hazard. Mater.* 179 (2010) 43–48.
- [42] S. Cengiz, L. Cavas, A promising evaluation method for dead leaves of *Posidonia oceanica* (L.) in the adsorption of methyl violet, *Mar. Biotechnol.* 12 (2010) 728–736.
- [43] C. Duran, D. Ozdes, A. Gundogdu, H.B. Senturk, Kinetics and isotherm analysis of basic dyes adsorption onto almond shell (*Prunus dulcis*) as a low cost adsorbent, *J. Chem. Eng. Data* 56 (2011) 2136–2147.
- [44] M.K. Dahri, M.R.R. Kooch, L.B.L. Lim, Removal of methyl violet 2B from aqueous solution using *Casuarina equisetifolia* needle, *ISRN Environ. Chem.* (2013), doi: [10.1155/2013/619819](https://doi.org/10.1155/2013/619819).
- [45] S. Lagergren, About the theory of so-called adsorption of soluble substances, *R. Swed. Acad. Sci.* 24 (1898) 1–39.
- [46] Y.S. Ho, G. McKay, Pseudo-second order model for sorption processes, *Process. Biochem.* 34 (1999) 451–465.
- [47] W.J. Weber, J.C. Morris, Kinetics of adsorption on carbon from solution, *J. Sanit. Eng. Div.* 89 (1963) 31–59.
- [48] Y. Zhao, Q. Yue, Q. Li, X. Xu, Z. Yang, X. Wang, B. Gao, H. Yu, Characterization of red mud granular adsorbent (RMGA) and its performance on phosphate removal from aqueous solution, *Chem. Eng. J.* 193–194 (2012) 161–168.
- [49] M. Özacar, I.A. Sengil, Application of kinetic models to the sorption of disperse dyes onto alunite, *Colloids Surf., A* 243 (2004) 105–113.
- [50] K. Lammers, G. Arbuckle-Keil, J. Dighton, FT-IR study of the changes in carbohydrate chemistry of three New Jersey pine barrens leaf litters during simulated control burning, *Soil Biol. Biochem.* 41 (2009) 340–347.
- [51] R. Xu, S. Xiao, J. Yuan, A. Zhao, Adsorption of methyl violet from aqueous solutions by the biochars derived from crop residues, *Bioresour. Technol.* 102 (2011) 10293–10298.